A single pair of pharyngeal neurons functions as a commander to reject high salt in *Drosophila melanogaster*

Jiun Sang[1,3], Subash Dhakal[1,3], Bhanu Shrestha[1], Dharmendra Kumar Nath[1], Yunjung Kim[1], Anindya Ganguly[2], Craig Montell[2,*], and Youngseok Lee[1,4,*]

[1]Department of Bio and Fermentation Convergence Technology, Kookmin University, Seoul, 02707, Republic of Korea

[2]Neuroscience Research Institute and Department of Molecular, Cellular and Developmental Biology, University of California, Santa Barbara, Santa Barbara, CA United States

[3]These authors contributed equally

[4]Lead Contract

[*]correspondence email, cmontell@ucsb.edu; or ylee@kookmin.ac.kr

ORCID ID: CM, 0000 0001 5637 1482; YL, 0000 0003 0459 1138

Abstract

Salt is an essential nutrient for survival, while excessive NaCl can be detrimental. In the fruit fly, *Drosophila melanogaster*, internal taste organs in the pharynx are critical gatekeepers impacting the decision to accept or reject a food. Currently, our understanding of the mechanism through which pharyngeal gustatory receptor neurons (GRNs) sense high salt are rudimentary. Here, we found that a member of the ionotropic receptor family, *Ir60b*, is expressed exclusively in a pair of GRNs activated by high salt. Using a two-way choice assay (DrosoX) to measure ingestion volume, we demonstrate that IR60b and two coreceptors IR25a and IR76b, are required to prevent high salt consumption. Mutants lacking external taste organs but retaining the internal taste organs in the pharynx exhibit much higher salt avoidance than flies with all taste organs but missing the three IRs. Our findings highlight the vital role for IRs in a pharyngeal GRN to control ingestion of high salt.

Introduction

The sense of taste enables animals to find nutritious food while avoiding potentially harmful substances in their environment. Most animals have evolved sophisticated systems to detect and steer clear of consuming levels of substances that are toxic. Salts such as NaCl are essential for a wide array of physiological functions. However, consumption of excessive salt can contribute to various health issues in mammals, including hypertension, osteoporosis, gastrointestinal cancer, autoimmune diseases, and can lead to death [1-6]. Therefore, high concentrations of salt are rejected by most animals.

Multiple studies have delved into how Na^+ is sensed in the *Drosophila* taste system, shedding light on the mechanisms behind the attraction to low salt and aversion to high salt [7-14]. The largest taste organs in flies are two bilaterally symmetrical labella, each of which is decorated with 31 gustatory bristles (sensilla). These sensilla are defined based on size (small, S; intermediate, I; large, L). The I-type sensilla harbor two gustatory receptor neurons (GRNs), while the S- and L-sensilla contain four. These GRNs fall into five classes (A-E) based on their response profiles [15]. These include Class A GRNs (formerly sugar GRNs; marked by *Gr5a* or *Gr64f*) [16,17], which respond to attractive compounds such as low salt, sugars, glycerol, fatty acids and carboxylic acids, Class B GRNs (formerly bitter GRNs; marked by *Gr66a*) [16,17], which are activated by high Na^+, bitter compounds, acids, polyamines, tryptophan, and L-canavanine, Class C GRNs respond to water (marked by *ppk28*) [18], Class D GRNs detect high levels of cations such as Na^+, K^+ and Ca^{2+} (marked by *ppk23*) [11,19], and Class E GRNs sense low Na^+ levels and pheromones

(marked by *Ir94e*) [11,20].

Several of the 66 ionotropic receptor (IR) family members function in the sensation of low and high salt. These include IR76b and IR25a, which are IR-coreceptors, and therefore have broad roles in sensing many taste stimuli including low and high Na^+ (also referred to in this work as salt) [7,8,10-12], Ca^{2+} [19], several carboxylic acids [21-23], fatty acids [24-27], amino acids [28], and carbonation [29]. A subset of Class A GRNs, as well as glutamatergic Class E GRNs are responsible for sensing low salt [8,11,12,15], and this sensation depends on IR56b working together with the broadly expressed co-receptors IR25a and IR76b [8]. Conversely, detection of high salt depends on Class B GRNs and Class D GRNs, and IR7c, in conjunction with IR25a and IR76b [7]. Additionally, two Pickpocket channels, Ppk11, Ppk19, and Sano have been associated with high salt aversion [30,31].

In addition to the labellum and taste bristles on other external structures, such as the tarsi, fruit flies are endowed with hairless sensilla on the surface of the labellum (taste pegs), and three internal taste organs lining the pharynx, the labral sense organ (LSO), the ventral cibarial sense organ (VCSO), and the dorsal cibarial sense organ (DCSO), which also function in the decision to keep feeding or reject a food [32-36]. A pair of GRNs in the LSO express a member of the gustatory receptor family, *Gr2a*, and knockdown of *Gr2a* in these GRNs impairs the avoidance to slightly aversive levels of Na^+ [14]. Pharyngeal GRNs also promote the aversion to bitter tastants, Cu^{2+}, L-canavanine, and bacterial lipopolysaccharides [37-40]. Other pharyngeal GRNs are stimulated by sugars and contribute to sugar consumption [32,36,41]. Remarkably, a pharyngeal GRN in each of the two LSOs functions in the rejection rather the acceptance of sucrose [42].

In this work, we investigated whether IRs function in pharyngeal GRNs for avoidance of high Na^+. We found that IR60b, along with co-receptors IR25a and IR76b function in a taste organ in the pharynx for limiting high salt consumption. *Ir60b* is expressed exclusively in a pair of pharyngeal GRNs in the LSO [42], and we found that these neurons respond to high Na^+. While these *Ir60b* GRNs are narrowly tuned, surprisingly, they have previously been shown to respond to sucrose and glucose [42]. Introduction of the rat capsaicin receptor, TRPV1 [43], into *Ir60b* GRNs induces aversion towards capsaicin, supporting the conclusion that *Ir60b*-positive GRNs are sufficient for instinctive avoidance. To validate these findings further, we used a two-way choice DrosoX assay [44] to measure actual ingestion levels. We found that the three *Ir* mutants consumed high salt at levels similar to sucrose over an extended period, emphasizing the critical role of this single pair of pharyngeal GRNs in controlling harmful ingestion of high salt.

Results

***Ir60b* functions in the repulsion to high salt**

To identify potential salt sensors in *Drosophila melanogaster*, we conducted binary food choice assays using 30 *Ir* mutants (***Figure 1A and Figure 1—figure supplement 1A***). Through screens in which we gave flies a choice between 2 mM sucrose alone or 2 mM sucrose plus a low, attractive level of salt (50 mM NaCl), we confirmed that *Ir76b* [12], *Ir25a*, and *Ir56b* [8], are essential for detecting low salt (***Figure 1—figure supplement 1A***). Moreover, using tip recordings to assay tastant-induced action potentials, we confirmed a previous report [8] that loss of *Ir56b* nearly

eliminated spikes in S-type and L-type sensilla in response to low salt (***Figure 1—figure supplement 1B***). Using *Ir56b-GAL4* to drive *UAS-mCD8*::*GFP,* we also confirmed that the reporter was restricted to a subset of Class A GRNs, which were marked with *LexAop-tdTomato* expressed under the control of the *Gr64f-LexA* (***Figure 1—figure supplement 1D—F***). We generated a *UAS-Ir56b* transgene which restored normal frequencies of action potentials in *Ir56b*-expressing GRNs (***Figure 1—figure supplement 1B***). Moreover, ectopic expression of *UAS-Ir56b* in GRNs that typically have minimal responses to low salt, caused a large increase in salt-induced action potentials (***Figure 1—figure supplement 1C***).

In our behavioral screen for *Ir* mutants required for avoiding high salt (300 mM NaCl), we found that in addition to *Ir7c*, *Ir25a*, and *Ir76b* as previously described [7], *Ir60b* was also required (***Figure 1A***). The *Ir60b* mutant, $Ir60b^{3}$, was generated by removing 768 base pairs, which spanned from 44 base pairs upstream of the predicted transcription start site to the region coding for the N-terminal 241 residues of the 577-amino acid protein (***Figure 1—figure supplement 2A—C***). We verified the impairment in high salt avoidance using a previously described mutant, $Ir60b^{1}$ (***Figure 1—figure supplement 2D***) [42]. We conducted dose-response behavioral assays using the *Ir60b* mutants, as well as *Ir25a*, *Ir76b* and *Ir7c* mutants and found that all four exhibited significant deficiencies in avoiding salt concentrations ranging from 200 mM to 500 mM (***Figure 1B***). Nevertheless, all of the mutants exhibited a strong aversion to an extremely high salt concentration (1000 mM), a level twice as concentrated as sea water. This very high level of NaCl could potentially trigger activation of nociceptive neurons, serving as a protective mechanism to prevent potential tissue and organ damage.

Activation of *Ir60b* neurons inhibits motivation to feed

To investigate whether activation of *Ir60b* GRNs induces aversive behavior, we used both chemogenetic and optogenetic approaches. Capsaicin, a ligand for the mammalian TRPV1 channel [43], does not normally elicit responses in flies (***Figure 1C***) as described previously [45]. Therefore, we expressed *UAS-trpV1* under the control of the *Ir60b-GAL4*, and presented the flies with a choice between a 2 mM sucrose and a 2 mM sucrose laced with 100 μM capsaicin. We found that the transgenic flies actively avoided capsaicin (***Figure 1C***), whereas expression of TRPV1 in Class A (sweet) GRNs (*Gr64f-GAL4* and *UAS-trpV1*) induced a preference for capsaicin (***Figure 1C***). These findings support the idea that the activation of *Ir60b* neurons leads to gustatory avoidance.

To further test the proposal that *Ir60b*-positive GRNs elicit aversive behavior, we expressed CsChrimson, a light-activated cation channel [46] in the *Ir60b* GRN. As controls we drove *UAS-CsChrimson* expression using either the *Gr5a-GAL4* or the *Gr66a-GAL4*. Upon stimulation with red lights and 2% sucrose, nearly all of the control flies (*UAS-CsChrimson* only) or flies expressing *UAS-CsChrimson* in Class A GRNs (*Gr5a-GAL4*) extended their proboscis (***Figure 1D***). In contrast, the PER was notably diminished in flies expressing *UAS-CsChrimson* in the Class B GRNs (*Gr66a-GAL4*) or in the *Ir60b* GRN (*Gr66a-GAL4*; 56.7 ± 4.2% and *Ir60b-GAL4*; 55.0 ± 5.0%, respectively; ***Figure 1D***). These results are fully consistent with a previous study showing optogenetic activation of the *Ir60b* GRN reduces consumption of a sugar [42]. Together, these findings provide compelling evidence that stimulation of the *Ir60b* GRN induces behavioral aversion.

***Ir60b* is not required in the labellum to sense high salt**

To investigate the physiological responses of labellar sensilla to high salt (300 mM), we conducted tip recordings on each of the 31 sensilla (***Figure 2A***). Five sensilla, including three S-type (S3, S5, and S7) and two L-type (L3 and L4), exhibited the strongest responses to high salt (***Figure 2—figure supplement 1A***). These responses were largely dependent on the IR25a and IR76b co-receptors, as well as IR7c (***Figure 2B, C and Figure 2—figure supplement 1B***) as reported [7]. Interestingly, the *Ir60b*^{3} deletion mutant did not affect the neuronal responses to high salt in labellar taste bristles (***Figure 2B and C***). We inactivated individual GRNs by expressing the inwardly rectifying K^+ channel (*UAS-Kir2.1*) [47] in Class A GRNs (*Gr64f-GAL4*) [48], Class B GRNs (*Gr66a-GAL4*) [17], Class C GRNs (*ppk28-GAL4*) [18], and Class D GRNs (*ppk23-GAL4*) [19], and confirmed that the aversive behavior and neuronal responses to high salt primarily relied on Class B and D GRNs (***Figure 2D and E***) as described [11].

To examine the gustatory repulsion to high salt that is mediated through the labellum, we conducted proboscis extension response (PER) assays. Starved control and *Ir* mutant flies extend their proboscis when the labellum is lightly touched with a 100 mM sucrose probe ***(Figure 2F***). Upon a second sucrose offering, the various fly lines exhibited slightly diminished responses (***Figure 2G***). When we added 300 mM salt to the sucrose, it significantly reduced the PER in the control group (***Figure 2H and I***; first offering 40.9 ± 4.0%; second offering 41.5 ± 3.7%). Both the *Ir25a*^{2} and *Ir76b*^{1} mutants also exhibited suppressed PERs, but the suppression was not as great as in the control ***(Figure 2H and I***). In contrast, high

salt reduced the PER by the *Ir60b*^{3} mutant to a similar extent as the control (***Figure 2H and I***; first offering 41.6 ± 6.5%; second offering 47.7 ± 6.7%). This indicates that the labellum of the *Ir60b*^{3} detects 300 mM salt normally, even though the mutant is impaired in avoiding high salt in a two-way choice assay (***Figure 1A***).

High salt sensor in the pharynx

The observations that *Ir60b* is required for the normal aversion to high salt, but does not appear to function in labellar bristles raise the possibility that *Ir60b* is required in the pharynx for salt repulsion. *Ir60b* is expressed in the pharynx where it plays a role in limiting sucrose consumption [42]. *Gr2a* is also expressed in the pharynx and contributes to the repulsion to moderate salt levels (150 mM) [14]. However, the *Gr2a*^{GAL4} mutant displays a normal response to high salt (450 mM) [14]. In our two-way choice assay, which focuses on 300 mM NaCl, we found that salt repulsion displayed by the *Gr2a*^{GAL4} mutant was also indistinguishable from the control (***Figure 2—figure supplement 2***).

To investigate a role for GRNs in the pharynx for high salt (300 mM) repulsion, we conducted tests on the *Poxn* mutant (*Poxn*$^{70\text{-}28}$/*Poxn*$^{\Delta M22\text{-}B5}$) in which external chemosensory bristles have been converted to mechanosensory sensilla [49]. The *Poxn* mutants retain GRNs in taste pegs, which are hairless sensilla [36]. As a result, *Poxn* mutants only possess intact internal gustatory organs, as well as taste pegs. We found that the aversive behavior to high salt was reduced in the *Poxn* mutants relative to the control (***Figure 2J***), consistent with previous studies demonstrating roles for GRNs in labellar bristles in high salt avoidance [7,11,12]. However, the diminished high salt avoidance of the *Poxn* mutant was significantly different from

the *Poxn*;*Ir60b*^{3} double mutant, even though the response of *Poxn*;*Ir60b*^{3} was not significantly different from *Ir60b*^{3} (***Figure 2J***).

Quantification of increased high salt ingestion in *Ir60b* mutants

In a prior study, it was observed that the repulsion to high salt exhibited by the *Ir60b* mutant was indistinguishable from wild-type [42]. Specifically, the flies were presented with a drop of liquid (sucrose plus salt) at the end of a probe, and the *Ir60b* mutant flies fed on the food for the same period of time as control flies [42]. However, this assay did not discern whether or not the volume of the high salt-containing food consumed by the *Ir60b* mutant flies was reduced relative to control flies. Therefore, to assess the volume of food ingested, we used the DrosoX system, which we recently developed (***Figure 3—figure supplement 1A***) [44]. This system consists of a set of five separately housed flies, each of which is exposed to two capillary tubes with different liquid food options. One capillary contained 100 mM sucrose and the other contained 100 mM sucrose mixed with 300 mM NaCl. The volume of food consumed from each capillary was then monitored automatically over the course of 6 hours and recorded on a computer. We found that control flies consuming approximately four times more of the 100 mM sucrose than the sucrose mixed with 300 mM NaCl (***Figure 3A***). In contrast, the *Ir25a*, *Ir60b*, and *Ir76b* mutants consumed approximately two-fold less of the sucrose plus salt (***Figure 3A***). Consequently, they ingested similar amounts of the two food options (***Figure 3B***; ingestion index). Thus, while the *Ir60b* mutant and control flies spend similar amounts of time in contact with high salt-containing food when it is the only option [42], the mutant consumes considerably less of the high salt food when presented with a

sucrose option without salt.

To further investigate the requirement for *Ir25a*, *Ir60b*, and *Ir76b*, we performed genetic rescue experiments. We introduced their respective wild-type cDNAs under the control of their cognate *GAL4* drivers, which resulted in a conversion from salt-insensitive behavior to the salt-sensitive behavior observed in wild-type flies (***Figure 3C-H***). In addition, the defects in the *Ir25a*^{2} and *Ir76b*^{1} mutants were fully rescued by expressing the wild-type *Ir25a* and *Ir76b* transgenes, respectively, in the pharynx using the *Ir60b-GAL4* (***Figure 3I-L***). This suggests that both IR25a and IR76b act as coreceptors in the *Ir60b* GRNs. Furthermore, we investigated whether the expression of *UAS-Ir60b* driven by *Ir25a-GAL4* or *Ir76b-GAL4* could rescue the defects observed in *Ir60b*^{3}. Despite the broad expression of *Ir60b* using these *GAL4* drivers, the *Ir60b* salt ingestion defect was rescued (***Figures 3M and N***).

Next, we addressed whether *Ir60b* is required specifically for regulating ingestion of high salt. To investigate this, we assessed the volumes of caffeine, strychnine, and coumarin consumed by *Ir60b*^{3} flies. We found that the *Ir60b*^{3} mutant displayed similar consumption patterns to the wild-type control flies for these bitter compounds (***Figure 3O, P and Figure 3—figure supplement 1B—E***). This is in contrast to the impairments exhibited by the *Gr66a*^{ex83} mutant (***Figure 3O, P and Figure 3—figure supplement 1B—E***), which displays defects in sensing many bitter chemicals. This indicates that *Ir60b* is involved in regulating the avoidance of high salt ingestion rather than general avoidance responses to toxic compounds. Nevertheless, the role of *Ir60b* in suppressing feeding is not limited to high salt, since *Ir60b* also functions in the pharynx in inhibiting the consumption of sucrose [42].

To investigate the aversion induced by high salt in the absence of a highly attractive sugar, such as sucrose, we combined 300 mM salt with 100 mM sorbitol, which is a tasteless but nutritive sugar [50,51]. Using two-way choice assays, we found that the *Ir25a*, *Ir60b*, and *Ir76b* mutants exhibited substantial reductions in high salt avoidance (***Figure 3—figure supplement 2A***). In addition, we performed DrosoX assays using 100 mM sorbitol alone or sorbitol mixed with 300 mM NaCl. Sorbitol alone provoked less feeding than sucrose since it is a tasteless sugar (***Figure 3—figure supplement 2B and C***). Nevertheless, addition of high salt to the sorbitol reduced food consumption (***Figure 3—figure supplement 2B and C***).

A single neuron in the LSO depends on *Ir25a*, *IR60b* and *Ir76b* for responding to both high salt and sucrose

In addition to *Ir60b*, two broadly required *Ir*s (*Ir25a* and *Ir76b*) also function in repulsion to high salt [11,12]. Moreover, we found that we could rescue the *Ir25a*, *Ir60b* or *Ir76b* DrosoX phenotypes using the same *Ir60b-GAL4* to drive expression of the cognate wild-type transgenes in the corresponding mutant backgrounds. These findings imply that all three *Ir*s are coexpressed in the *Ir60b* GRN in the pharynx. Therefore, we examined the relative expression patterns of the *Ir60b-GAL4* reporter with the *Ir25a* and *Ir76b* reporters. We observed that the *Ir76b-QF* reporter was expressed in two cells within the labral sensory organ (LSO), one of which colocalized with the *Ir60b* reporter (***Figure 4A***). Additionally, the expression pattern of the *Ir25a-GAL4* perfectly overlapped with that of *Ir76b-QF* in the LSO (***Figure 4B***). Thus, we suggest that *Ir25a*, *Ir60b* and *Ir76b* function in the same GRN in the LSO to limit consumption of high salt. We attempted to induce salt activation in the I-type

sensilla by ectopically expressing *Ir60b*, under control of the *Gr33a-GAL4*. *Gr33a* is co-expressed with *Gr66a* [52], which has been shown to be co-expressed with *Ir25a* and *Ir76b* [19,53]. When we performed tip recordings from I5 and I9 sensilla, we did not observe a significant increase in action potentials in response to 300 mM NaCl (***Figure 4—figure supplement 1A***), indicating that ectopic expression of *Ir60b* in combination with *Ir25a* and *Ir76b* is not sufficient to generate a high salt receptor.

To determine whether the *Ir60b* GRN in the LSO is activated by high salt, we examined Ca^{2+} responses in the LSO using *UAS-GCaMP6f*, expressed under the control of each *GAL4* driver. In the wild-type LSO, we identified a single cell that responded to 300 mM NaCl (***Figure 4C***), indicating that the GRN in the LSO that expresses all three reporters responds to high salt. Moreover, this GRN responded robustly to 300 mM to 1000 mM Na^+ but not to a low level of Na^+ (50 mM; ***Figure 4E***). We then examined the Ca^{2+} responses in the *Ir25a*^{2}, *Ir60b*^{3}, and *Ir76b*^{1} mutants, and found that each of them failed to respond to NaCl (***Figure 4D and E***). Additionally, we rescued the deficits in the GCaMP6f responses exhibited by each mutant by expressing a wild-type transgene under control of the corresponding *GAL4* driver (***Figure 4F***). We also tested other Cl^- salts ($CaCl_2$, $MgCl_2$, and KCl) to determine if Cl^- rather than Na^+ induced responses in the *Ir60b* GRN. None of these other salts affected these neurons at the 50 mM, 300 mM, and 500 mM concentrations tested (***Figure 4G***). In contrast, NaBr induced GCaMP6f responses (***Figure 4H***). Thus, the *Ir60b* GRN is responsive to Na^+ and not Cl^-. Due to the effects of NaBr on the *Ir60b* GRN, we used the DrosoX assay to determine whether 300 mM NaBr suppressed ingestion of sucrose. We found that the impact of NaBr on sucrose ingestion was similar to that with NaCl (***Figure 4—figure supplement 1B and C***). We also found

that the *Ir60b* GRN did not respond to bitter compounds such as quinine, caffeine, strychnine, lobeline, denatonium, and coumarin at the 5 mM and 50 mM concentrations (***Figure 4I***).

It has been shown previously that *Ir60b* is required in a single GRN in the LSO for suppressing sucrose feeding, and this neuron responds to sucrose [42]. Therefore, we tested whether the same GRN in the LSO that responds to salt also responds to sucrose. Using GCaMP6f, we found that the *Ir60b* GRN was responsive to sucrose in the LSO of control flies, but not in the *Ir25a*, *Ir60b* and *Ir76b* mutants (***Figure 4J***). Furthermore, we used GCaMP6f to compare the Ca^{2+} responses exhibited by the *Ir60b* GRN to 100 mM sucrose alone, 300 mM NaCl alone, and a combination of 100 mM sucrose and 300 mM NaCl. We found that the Ca^{2+} responses were significantly higher when we exposed the *Ir60b* GRN to 300 mM NaCl alone, compared with the response to 100 mM sucrose alone (***Figure 4—figure supplement 1D***). However, the GCaMP6f response was not higher when we presented 100 mM sucrose in combination with 300 mM NaCl, compared with the response to 300 mM NaCl alone. We conclude that the same LSO neuron depends on the same three receptors (IR25a, IR60b, and IR76b) for suppressing feeding in response to high salt or to sucrose.

Both Class B and Class D GRNs in labellar bristles respond to high salt [15], and the Class D GRNs (marked by *ppk23*) depend on *Ir7c* as well as *Ir25a* and *Ir76b* for responding to high salt [7]. Consequently, we investigated whether *Ir7c* plays a role in the *Ir60b* GRN in the LSO. We expressed *UAS-GCaMP6f* under control of the *Ir60b-GAL4* in either or $Ir7c^{GAL4}$ mutant background or in a heterozygous ($Ir7c^{GAL4}$/+) control. We then stimulated the *Ir60b* GRN in the LSO with 300 mM NaCl and found

that the responses elicited by the mutant and control were the same (***Figure 4—figure supplement 2A***). Consistent with these findings, we did not detect *Ir7c* reporter expression in the *Ir60b* GRNs (***Figure 4—figure supplement 2B—D***).

Discussion

The taste organs lining the walls of the pharynx represent the final gatekeepers that flies use to decide whether to continue feeding or to reject the food. We found that activation of a single pharyngeal GRN by high salt depends on three IRs, two of which are widely expressed in other GRNs (*Ir25a* and *Ir76b*) and were previously shown to function in salt taste sensation in external labellar bristles. In addition, we identified a third IR (*Ir60b*) that contributes to salt rejection. Consistent with a previous study [42], *Ir60b* is expressed in a single GRN in each of two labral sense organs (LSOs) lining the pharynx. In addition, we demonstrated that *Ir60b* is co-expressed with *Ir25a* and *Ir76b* in this one GRN in each LSO.

Multiple observations in this study underscore the important role of the *Ir60b* GRN in sensing high Na^+ levels and in promoting salt rejection. Mutation of *Ir60b* eliminates the flies ability to reject sucrose laced with high salt over another option with sucrose only. This result is especially notable in view of the observation that flies that are missing all GRNs in labellar bristles in the *Poxn* mutant exhibit a less pronounced defect than the *Ir60b* mutant, since *Poxn* mutant flies still retain some bias for sucrose over sucrose laced with high salt. The observation that one pair of pharyngeal GRNs is sufficient to induce rejection of high salt underscores the profound role of internal taste neurons in protecting flies from ingesting dangerous

levels of this mineral. In addition, activation of the *Ir60b* GRN suppresses feeding since optogenetic activation of these neurons effectively suppresses the proboscis extension response (PER) when the flies are presented with a highly attractive tastant (sucrose). Conversely, Yang et al. demonstrated that activation of *Ir60b* neurons can induce the activation of IN1 neurons, potentially leading to heightened feeding [54]. However, our research reveals a specific activation pattern for *Ir60b* neurons. Instead of being generalists, they exhibit specialization for certain sugars, such as sucrose and high salt. As a result, while *Ir60b* GRNs activate IN1 neurons [54], we posit that there are other neurons in the brain responsible for inhibiting feeding.

A finding that is seemingly conflicting with the optogenetic results is that mutation of *Ir60b* does not reduce the suppression of the PER when the flies are presented with sucrose laced with high Na^+ levels. The PER assay under high salt conditions only permits flies to taste the food without allowing ingestion. Consequently, the internal sensor may not exhibit suppression of the PER. In contrast, optogenetic activation has the capability to directly stimulate the internal sensor, leading to the induction of PER suppression. We propose that high Na^+ is effective in suppressing the PER by the *Ir60b* mutant since these flies still have functional high salt receptors in aversive GRNs in labellar bristles. In support of this conclusion, loss of either *Ir25a* or *Ir76b* reduces the suppression of the PER by high salt, and this occurs because *Ir76b* and *Ir25a* are required in both high salt activated GRNs in labellar bristles [11,12] and in the *Ir60b* GRN in the pharynx.

We also found that the requirement for *Ir60b* appears to be different when performing binary liquid capillary assay (DrosoX), versus solid food binary feeding assays. When we employed the DrosoX assay to test mutants that were missing salt

aversive GRNs in labellar bristles but still retained functional *Ir60b* GRNs, the flies behaved the same as wild-type flies (e.g. ***Figure 3J and L***). However, using solid food binary assays, *Poxn* mutants, which are missing labellar taste bristles but retain *Ir60b* GRNs [36], displayed repulsion to high salt food that was intermediate between control flies and the *Ir60b* mutant (***Figure 2J***). *Poxn* mutants still possess taste pegs [36], and these hairless taste organs become exposed to food only when the labial palps open. We suggest that there are high-salt sensitive GRNs associated with taste pegs, which are accessed when the labellum contacts a solid substrate, but not when flies drink from the capillaries used in DrosoX assays. This explanation would also account for the findings that the *Ir60b* mutant is indifferent to 300 mM NaCl in the DrosoX assay (***Figure 3B***), but prefers 1 mM sucrose alone over 300 mM NaCl and 5 mM sucrose in the solid food binary assay (***Figure 1B***). Alternatively, the different behavioral responses might be due to the variation in sucrose concentrations in each of these two assays, which employed 5 mM sucrose in the solid food binary assay, as opposed to 100 mM sucrose in the DrosoX assay. The disparity in attractive valence between these two concentrations of sucrose might consequently impact feeding amount and preference.

Another unresolved question is why does the some pharyngeal GRN respond to sucrose and high Na^+. It has been pointed out that since flies prefer over ripe fruit, which has lower sucrose levels that ripe fruit, then activation of the *Ir60b* GRN by sucrose might serve to favor consumption of fruit at an advanced state of ripeness [37]. In contrast to sugar, Na^+ levels tend to remain constant during the ripening process [55] and remain at relatively low levels (50-100mM), which is below the level that is aversive to flies. Thus, in contrast to sucrose, assessing the concentration of Na^+

does not aid in the distinction of ripe versus overripe fruit, but may be important in avoiding consuming non-vegetarian sources of food that are high in Na^+.

Based on Ca^{2+} imaging results with GCaMP6f, we conclude that the *Ir60b* GRN directly responds to NaCl, and this depends on the presence of *Ir25a*, *Ir60b* and *Ir76b*. The *Ir60b* GRN responds to high NaCl, but is not stimulated by $CaCl_2$, $MgCl_2$ and KCl. Thus, the *Ir60b* GRN is a Na^+ sensor not a Cl^- sensor. In further support of this conclusion, we found that the *Ir60b* GRN also responds to NaBr.

An open question is the subunit composition of the pharyngeal high Na^+ receptor, and whether the sucrose/glucose and Na^+ receptors in the *Ir60b* GRN are the same or distinct. Our results indicate that the high salt sensor in the *Ir60b* GRN includes IR25a, IR60b and IR76b since all three IRs are required in the pharynx for sensing high levels of NaCl. I-type sensilla do not elicit a high salt response, and we were unable to induce salt activation in I-type sensilla by ectopically expressing *Ir60b*, under control of the *Gr33a-GAL4.* This indicates that IR25a, IR60b and IR76b are insufficient for sensing high Na^+. The inability to confer a salt response by ectopic expression of *Ir60b* was not due to absence of *Ir25a* and *Ir76b* in *Gr33a* GRNs since *Gr33a* and *Gr66a* are co-expressed [52], and *Gr66a* GRNs express *Ir25a* and *Ir76b* [19,53]. Thus, the high salt receptor in *Ir60b* GRNs appears to require an additional subunit. Given that Na^+ and sugars are structurally unrelated, we suggest that the Na^+ and sucrose/glucose receptors do not include the identical set of subunits, or that they activate a common receptor through disparate sites.

Finally, it is remarkable that the single *Ir60b* GRN in the LSO of the pharynx is also stimulated by sucrose and to a lesser extent to glucose [42], since this GRN is otherwise very narrowly tuned. We did not detect GCaMP signals upon application

any of six bitter tastants tested. The *Ir60b* GRN is also unresponsive to trehalose and glycerol. Based on behavioral experiments, mutation of *Ir60b* does not impact on consumption of an array of amino acids, low pH, bitter chemicals and other sugars [37]. It is also surprising that the pharyngeal GRN that responds to Na^+ is unresponsive to other cations such as Ca^{2+}, which is toxic at high levels [19]. The fact that there are relatively few pharyngeal GRNs, yet one is narrowly tuned to sucrose, glucose and Na^+ underscores the critical role of limiting Na^+ consumption in flies, which could otherwise lead to dehydration, and dysfunction of many homeostatic processes impacted by excessive levels of Na^+ [56].

Materials and methods

Key resources table

Reagent type	Designation	SOURCE	IDENTIFIER
Antibody	Mouse anti-GFP	Molecular probes	Cat # A11120; RPID: AB_221568
Antibody	Rabbit anti-DsRed	Clontech	Cat # 632496; RPID: AB_10013483
Antibody	Goat Anti-mouse Alexa Fluro 488	Invitrogen	Cat # A32723; RRID: AB_2633275
Antibody	Goat anti-rabbit Alexa Fluor 568	Invitrogen	Cat # A11011; RPID: AB_143157
Chemical compound	Sucrose	Sigma-Aldrich	Cat # 9378S
Chemical compound	Tricholine citrate	Sigma-Aldrich	Cat # T0252
Chemical compound	Sulforhodamine B	Sigma-Aldrich	Cat # 230162
Chemical compound	Capsaicin	Sigma-Aldrich	Cat # M2028
Chemical compound	Caffeine	Sigma-Aldrich	Cat # C02750
Chemical compound	$CaCl_2$ dihydrate	Sigma-Aldrich	Cat # C3881
Chemical compound	KCl	Sigma-Aldrich	Cat # P9541
Chemical compound	Quinine	Sigma-Aldrich	Cat # Q1125
Chemical compound	Strychnine	Sigma-Aldrich	Cat # S8753
Chemical compound	Lobeline	Sigma-Aldrich	Cat # 141879

Chemical compound	Denatonium	Sigma-Aldrich	Cat # D5765
Chemical compound	Coumarin	Sigma-Aldrich	Cat # C4261
Chemical compound	Brilliant blue FCF	Wako Pure Chemical Industry	Cat # 027-12 842
Chemical compound	Paraformaldehyde	Electron Micro-scopy Sciences	Cat # 15710
Chemical compound	NaCl	LPS solution	Cat # NACL0 1
Chemical compound	$MgCl_2$ hexahydrate	SAMCHUN	Cat # M0038
Chemical compound	NaBr	DUKSAN	Cat # S2531
Chemical compound	Goat Serum, New Zealand origin	Gibco	Cat # 162100 64
Genetic reagent (*Drosophila melanogaster*)	w^{1118}	Bloomington Drosophila Stock Center (BDSC)	BDSC:5905
Genetic reagent (*Drosophila melanogaster*)	$Ir7a^{1}$	Dr. Y. Lee	[23]
Genetic reagent (*Drosophila melanogaster*)	$Ir7g^{1}$: $y^{1}w^{*}Mi\{y^{+mDint2}=MIC\}Ir7g^{MI06687}$	BDSC	BDSC:42420
Genetic reagent (*Drosophila melanogaster*)	$Ir7c^{GAL4}$	Dr. M. D. Gordon	[7]
Genetic reagent (*Drosophila melanogaster*)	$Ir8a^{1}$: $w^{*}TI\{w[+m^{*}]=TI\}Ir8a^{1};Bl^{1}L^{2}/CyO$	BDSC	BDSC:23842
Genetic reagent (*Drosophila melanogaster*)	$Ir10a^{1}$: $w^{1118}Mi\{GFP^{E.3xP3}=ET1\}Ir10a^{MB03273}$	BDSC	BDSC:41744
Genetic reagent (*Drosophila melanogaster*)	$Ir21a^{1}$: $w^{1118};PBac\{w^{+mC}=PB\}Ir21a^{c02720}$	BDSC	BDSC:*10975*
Genetic reagent (*Drosophila melanogaster*)	$Ir25a^{2}$	Dr. L. Vosshall	[57]
Genetic reagent (*Drosophila melanogaster*)	$Ir47a^{1}$	Dr. Y. Lee	[23]
Genetic reagent (*Drosophila melanogaster*)	$Ir48a^{1}$: $w^{1118};Mi\{GFP^{E.3xP3}=ET1\}Ir48a^{MB09217}$	BDSC	BDSC:26453
Genetic reagent (*Drosophila melanogaster*)	$Ir48b^{1}$: $w^{1118};Mi\{GFP^{E.3xP3}=ET1\}Ir48b^{MB02315}$	BDSC	BDSC:23473
Genetic reagent (*Drosophila melanogaster*) Genetic reagent (*Drosophila melanogaster*)	$Ir51b^{1}$: $w^{1118};PBac\{w^{+mC}=PB\}row^{c00387}$ I $r51b^{c00387}$ $Ir52a^{1}$	BDSC Dr. Y. Lee	BDSC:10046 [23]
Genetic reagent (*Drosophila melanogaster*)	$Ir52b^{1}$: $w^{1118};Mi\{GFP^{E.3xP3}=ET1\}Ir52b^{MB02231}/SM6a$	BDSC	BDSC:25212

Genetic reagent (*Drosophila melanogaster*)	*Ir52c*^{1}: *w*^{1118};Mi{GFP$^{E.3xP3}$=ET1}Ir52c^{MB04402}	BDSC	BDSC:24580
Genetic reagent (*Drosophila melanogaster*)	*Ir56a*^{1}	Dr. Y. Lee	[23]
Genetic reagent (*Drosophila melanogaster*)	*Ir56b*^{1}: *w*^{1118};Mi{GFP$^{E.3xP3}$=ET1}Ir56b^{MB09950}	BDSC	BDSC:27818
Genetic reagent (*Drosophila melanogaster*)	*Ir56d*^{1}: *w*;Ir56d*^{1}	BDSC	BDSC:81249
Genetic reagent (*Drosophila melanogaster*)	*Ir60b*^{1}	Dr. J. Carlson	[42]
Genetic reagent (*Drosophila melanogaster*)	*Ir60b*^{3}	Dr. Y. Lee	In this study
Genetic reagent (*Drosophila melanogaster*) Genetic reagent (*Drosophila melanogaster*)	*Ir62a*^{1}: y^{1}w*;Mi{y$^{+mDint2}$=MIC}Ir62a^{MI00895} Iml1^{MI00895}/TM3, Sb^{1} Ser^{1} *Ir67a*^{1}: y^{1}w*;Mi{y$^{+mDint2}$=MIC}Ir67a^{MI11288}	BDSC BDSC	BDSC:32713 BDSC:56583
Genetic reagent (*Drosophila melanogaster*)	*Ir75d*^{1}: *w*^{1118};Mi{GFP$^{E.3xP3}$=ET1}Ir75d^{MB04616}	BDSC	BDSC:*24205*
Genetic reagent (*Drosophila melanogaster*)	*Ir76b*^{1}	Dr. C. Montell	[12]
Genetic reagent (*Drosophila melanogaster*)	*Ir85a*^{1}: *w*^{1118};Mi{GFP$^{E.3xP3}$=ET1}Ir85a^{MB04613} Pif1A^{MB04613}	BDSC	BDSC:24590
Genetic reagent (*Drosophila melanogaster*)	*Ir92a*^{1}: *w*^{1118};Mi{GFP$^{E.3xP3}$=ET1}Ir92a^{MB03705}	BDSC	BDSC:23638
Genetic reagent (*Drosophila melanogaster*)	*Ir94a*^{1}	Dr. Y. Lee	[23]
Genetic reagent (*Drosophila melanogaster*)	*Ir94b*^{1}:*w*^{1118};Mi{GFP$^{E.3xP3}$=ET1}Ir94b^{MB02190}	BDSC	BDSC:23424
Genetic reagent (*Drosophila melanogaster*)	*Ir94c*^{1}	Dr. Y. Lee	[23]
Genetic reagent (*Drosophila melanogaster*)	*Ir94d*^{1}:y^{1}w*;Mi{y$^{+mDint2}$=MIC}Ir94d^{MI01659} CG17380^{MI01659}	BDSC	BDSC:33132
Genetic reagent (*Drosophila melanogaster*)	*Ir94f*^{1}: y^{1}w*;Mi{y$^{+mDint2}$=MIC}Ir94f^{MI00928}	BDSC	BDSC:33095
Genetic reagent (*Drosophila melanogaster*)	*Ir94g*^{1}: *w*^{1118};Mi{GFP$^{E.3xP3}$=ET1}Ir94g^{MB07445}	BDSC	BDSC:25551

Genetic reagent (*Drosophila melanogaster*)	*Ir94h*^{1}	Dr. Y. Lee	[23]
Genetic reagent (*Drosophila melanogaster*)	*Ir100a*^{1}: *w*^{1118};P{w^{+mC}=EP}Ir100a^{G19846} CG42233^{G19846}	BDSC	BDSC:31853
Genetic reagent (*Drosophila melanogaster*)	*UAS-mCD8*::*GFP*	BDSC	BDSC:5137
Genetic reagent (*Drosophila melanogaster*)	*UAS-mCD8*::*GFP*	BDSC	BDSC:32184
Genetic reagent (*Drosophila melanogaster*)	*UAS-Kir2.1*	BDSC	BDSC:6595
Genetic reagent (*Drosophila melanogaster*)	*UAS-Ir25a*	Dr. Y. Lee	[19]
Genetic reagent (*Drosophila melanogaster*)	*UAS-Ir60b*	Dr. Y. Lee	In this study
Genetic reagent (*Drosophila melanogaster*)	*UAS-Ir76b*	Dr. C. Montell	[12]
Genetic reagent (*Drosophila melanogaster*)	*Ir25a-GAL4*	Dr. L. Vosshall	[57]
Genetic reagent (*Drosophila melanogaster*)	*Ir60b-GAL4*	Dr. C. Montell	[42]
Genetic reagent (*Drosophila melanogaster*)	*Ir76b-GAL4*	Dr. C. Montell	[12]
Genetic reagent (*Drosophila melanogaster*)	*ppk23-GAL4*	Dr. K. Scott	[58]
Genetic reagent (*Drosophila melanogaster*)	*ppk28-GAL4*	Dr. H. Amrein	[18]
Genetic reagent (*Drosophila melanogaster*)	*Gr66a-GAL4*	Dr. H. Amrein	[17]
Genetic reagent (*Drosophila melanogaster*)	*Gr64f-GAL4*	Dr. A. Dahanukar	[19]
Genetic reagent (*Drosophila melanogaster*)	*Ir76b-QF*	BDSC	BDSC:51312
Genetic reagent (*Drosophila melanogaster*)	*QUAS-tdTomato*: *y*^{1}*w*^{1118}; P{QUAS-mtdTomato-3xHA}26	BDSC	BDSC:30005
Genetic reagent (*Drosophila melanogaster*)	*Poxn*$^{\Delta M22-B5}$: y^{1}w^{67c23}; Mi{ET1}Poxn^{MB00113}	BDSC	BDSC:22701

Genetic reagent (*Drosophila melanogaster*)	*Poxn*$^{70-28}$: *Poxn*^{70}/CyO; twi-Gal4, UAS -2XEGFP	BDSC	BDSC:60688
Software	Origin Pro Version	Dr. Y. Lee	https:/www.originlab.com
Software	GraphPad Prism	Dr. Y. Lee	https:/www.graphpd.com
Software	Autospike 3.1 software	Dr. Y. Lee	https://www.syntech.co.za/
Software	Fiji/ImageJ software	Dr. Y. Lee	https://fiji.sc
Software	ZEN lite 2.5 blue	Dr. Y. Lee	https://www.zeiss.com/

427

428 **Generation of *Ir60b*^{3} and *UAS-Ir60b* lines**

429 The *Ir60b*^{3} mutant was generated by ends-out homologous recombination [59]. For
430 generating the construct for injections, approximately two 3-kb genomic fragments
431 were amplified by PCR, and subcloned into *Not*I and *Bam*HI sites of the pw35 vector
432 [59]. The resulting mutation deleted the region from -44 to +724 (the A of the ATG
433 initiation codon is defined at +1). The construct was injected into *w*^{1118} embryos by
434 Best Gene Inc. We outcrossed the mutant to *w*^{1118} for six generations.

435 To generate the *UAS-Ir60b* transgenic line, we amplified the full-length *Ir60b*
436 cDNA by reverse transcription polymerase chain reaction (RT-PCR) using mRNA
437 prepared from whole adult flies and the following primer pair: 5'-
438 GAGAATTCAACTCGAAAATGAGGCGG-3' and 5'-
439 ATGCGGCCGCAATGCTAATTTTG-3'. The *Ir60b* cDNA was subcloned between the
440 *Eco*RI and *Not*I sites of the pUAST vector [60], and verified by DNA sequencing. The
441 p*UAS-Ir60b* vector was introduced into *w*^{1118} embryos by P-element mediated
442 germline transformation (Korea Drosophila Resource Center, Republic of Korea).

443

444 **Chemical reagents**

The following chemicals were purchased from Sigma-Aldrich (USA): sucrose (CAS No. 57-50-1), tricholine citrate (TCC) (CAS No. 546-63-4), sulforhodamine B (CAS No. 3520-42-1), capsaicin (CAS No. 404-86-4), caffeine (CAS No. 58-08-2), $CaCl_2$ dihydrate (CAS No. 10035-04-8), KCl (CAS No. 7447-40-7), quinine (CAS No. 6119-47-7), strychnine (CAS No. 1421-86-9), lobeline (CAS No. 134-63-4), denatonium (CAS No. 6234-33-6), and coumarin (CAS No. 91-64-5). Brilliant blue FCF (CAS No. 3844-45-9) was purchased from Wako Pure Chemical Industry (Japan). Paraformaldehyde (CAS No. 30525-89-4) was purchased from Electron Microscopy Sciences (USA). NaCl (CAS No. 7647-14-5) was purchased from LPS solution (Korea). NaBr (CAS No. 7647-15-6) was purchased from DUKSAN (Korea). Goat serum, New Zealand Origin was purchased from Gibco (USA).

Binary food choice assay using microtiter dishes

We conducted binary food choice assays as described [61]. Briefly, two mixtures were prepared, one of which consisted of 1% agarose, the indicated concentration of NaCl and 5 mM sucrose and red food dye (sulforhodamine B, 0.1 mg/ml). The second mixture contained 1% agarose, 1 mM sucrose, and blue food dye (Brilliant Blue FCF, 0.125 mg/ml). The same phenotypes in Figure 1B were verified by swapping the tastants/dye combinations. The two foods were distributed in alternating wells of a 72-well microtiter dish (Cat # 438733, Thermo Fisher Scientific, USA) in a zigzag pattern. 40–50 flies (3—6 days old) were starved for 18-hour on 1% agarose and transferred to the microtiter dish, which was placed in a dark and humid chamber for 90 mins. The flies were then frozen at -20°C, and the colors of their abdomen to determine the number of flies with blue (N_B), red (N_R), and purple (N_P) abdomens.

Preference indexes (P.I.s) were calculated using the following equation: $(N_R - N_B)/(N_R + N_B + N_P)$ or $(N_B - N_R)/(N_R + N_B + N_P)$, depending on the specific dye/tastant combinations. A P.I. of -1.0 or 1.0 indicates a complete preference for either 5 mM sucrose with the indicated concentration of NaCl or 1 mM sucrose alone, respectively. A P.I. of 0.0 indicates no preference between the two food alternatives.

Proboscis extension response (PER) assays

PER assays were conducted as described [62] with minor modifications. Briefly, 20—25 flies (3—6 days old) were deprived of food for 18—20 hrs in vials containing Kimwipe paper wet with tap water. After briefly anesthetizing the flies on ice, they were carefully trapped inside a pipette tip with a volume of 200 µL yellow tip. To expose their heads, the edge of the pipette tip was gently cut using a paper cutter blade. The protruded head and proboscis were used to deliver stimuli. Total 15—20 flies were prepared for the next step. To eliminate any potential biases due to thirst, water was initially provided to the flies with Kimwipe paper until they no longer responded to water. For both the positive control and initial stimulation, a 2% sucrose solution was used. Flies that did not exhibit a response to the sucrose during the initial exposure were excluded from the experiment. The same conditions as the initial exposures were maintained for the second exposure. Therefore, 10—18 flies were selected for the next step. The tastant stimuli, consisting of either 2% sucrose or 2% sucrose mixed with 300 mM NaCl, were presented using Kimwipe paper. We scored the PER as 1.0 with both complete extensions and partial extensions. PER was calculated using the following equation: (PER flies)/(selected flies). Each test round included 10-18 flies.

DrosoX binary capillary feeding assay

DrosoX is a recently developed modification of the Expresso technique, which quantifies the amount of feeding by fruit flies [63]. We conducted DrosoX assays essentially as described [44]. Each sensor bank of the DrosoX system is composed of a printed circuit board housing five Linear Optical Array Sensors (TAOS, TSL1406). Each sensor consists of 768 photodiodes and a microcontroller, establishing a connection to a computer through a Universal Serial Bus port. In the DrosoX setup, when a fly consumes liquid food from a glass capillary, a decrease in the liquid level is identified by a photodiode, enabling the calculation of instantaneous food ingestion. Photodiodes are semiconductor devices, which generate photocurrents upon absorbing light. To ensure light-tight conditions, the sensor bank is enclosed in a box made of black acrylic sheets using precision cutting. A computer reads the electrical signal generated by each photodiode, and the microcontroller (STMicroelectronics, STM32 F103RCBT6) on a development board (Scitech Korea) connected to the DrosoX sensor bank samples the light intensity at each pixel in the array at a rate of 8 Hz. Liquid level readings can be obtained at sample rates ranging from 0.1 to 2 Hz. The data acquisition software records the time vs. liquid level data for multiple sensor banks into a single file using the Hierarchical Data Format (HDF5) (http://www.hdfgroup.org/HDF5/). The obtained data is then analyzed using software (DrosoX_gui) supplied by Scitech Korea.

The conduct the DrosoX assays, we inserted the system in a controlled incubator (25°C, 60% humidity). To quantify ingestion, a mixture comprising 100 mM sucrose and the specified concentration of chemicals was injected into a glass tube

(Cat # 53432-706; VWR International, USA) using a syringe (KOVAX-SYRINGE 1 mL 26G; KOREA VACCINE, Korea) and needle (Cat # 90025; Hamilton, Switzerland). DrosoX was equipped with five glass tubes containing a solution, while DrosoXD was equipped with another set of five glass tubes containing different solutions (***Figure 3—figure supplement 1A***). DrosoX and DrosoXD were cross-tested. Each cuvette contained flies (3-6 days old) and was physically isolated to prevent them from consuming the solution prior to the experiment. Each experiment was conducted for a duration of 6 hours, from 9 AM to 3 PM. The ingestion amount at time X (X h) was calculated as the difference between the initial solution amount (0 h) and the solution amount at time X.

The ingestion index (I.I) was calculated at each time point using the following equation: (Ingestion $volume_{DrosoX}$ - Ingestion $volume_{DrosoXD}$)/(Ingestion $volume_{DrosoX}$ + Ingestion $volume_{DrosoXD}$) or (Ingestion $volume_{DrosoXD}$ - Ingestion $volume_{DrosoX}$)/(Ingestion $volume_{DrosoXD}$ + Ingestion $volume_{DrosoX}$), depending on the specific tastant combinations. A I.I. at 0.0 indicated no preference based on their ingestion between the two food alternatives.

Tip recordings to assay tastant-induced action potentials

To measure tastant-induced action potentials, we performed tip recordings as previously described [64]. We immobilized 3—6 day-old flies by exposing them to ice. We immobilized a fly by inserting a reference glass electrode filled with Ringer's solution through the back thorax all the way into the proboscis. The recording glass electrode (tip diameter 10—20 μm) contained the NaCl or aversive compounds dissolved in distilled water with 30 mM tricholine citrate (TCC) or 1 mM KCl as the

electrolyte. Reference glass electrode and recording glass electrode were created by processing Standard Glass Capillaries (Cat # IB150F-3, World Precision Instruments, USA) with glass puller. The recording electrode was placed over a bristle on the labellum and connected to a pre-amplifier (Taste PROBE, Syntech, Germany), which amplified the signals by a factor of 10 using a signal connection interface box (Syntech) and a 100-3,000 Hz band-pass filter. The recorded action potentials were acquired at a sampling rate of 12 kHz and analyzed using Autospike 3.1 software (Syntech). The average frequencies of action potentials (spikes/s) were based on spikes occurring between 50 and 550 msec after contact of the recording electrode. The sensilla bristles were defined as described [65].

Immunohistochemistry

We performed immunohistochemistry as previously described [66] with slight modifications. Labella were dissected from 6—8 day-old flies and fixed in a solution containing 4% paraformaldehyde (Electron Microscopy Sciences, Cat # 15710) and 0.2% Triton X-100 for 15 minutes at room temperature. The tissues were then washed three times with PBST (1x PBS and 0.2% Triton X-100), bisected using a razor blade, and incubated in blocking buffer (0.5% goat serum in 1x PBST) for 30 minutes at room temperature. To detect the target protein, primary antibodies (mouse anti-GFP; Molecular Probes, Cat # A11120; diluted 1:1,000 and rabbit anti-dsRed; Clontech, Cat # 632496; diluted 1:1,000) were added to fresh blocking buffer and incubated with the samples overnight at 4 °C. The tissues were then washed three times with PBST, incubated with the secondary antibodies (goat anti-mouse Alexa Fluor 488; Invitrogen, Cat # A32723; diluted 1:200 and goat anti-rabbit Alexa

Fluor 568; Invitrogen, Cat # A11011; diluted 1:200) for 4 hours at 4 °C, washed three times with PBST, and placed in 1.25x PDA mounting buffer (containing 37.5% glycerol, 187.5 mM NaCl, and 62.5 mM Tris pH 8.8). The signals were visualized using a Leica Stellaris 5 confocal microscope.

Ex vivo Ca^{2+} imaging using GCaMP6f

Ex vivo Ca^{2+} imaging was performed as previously described [67] with slight modifications using 6—8 day-old flies expressing *UAS-GCaMP6f* driven by *Ir25a-GAL4*, *Ir60b-GAL4* or *Ir76b-GAL4*, which were incubated at 25 °C, under 12 hr light/12 hr dark cycles and 50-60%, humidity. 0.5% low melting agarose was applied to a confocal dish (Cat # 102350, SPL LIFE SCIENCE, Korea). After solidification of the low-melting agarose, a blade was used to cut and create a shallow well for sample fixation. Fly heads were carefully decapitated using sharp razor blades, followed by excising a small portion of the extended proboscis to facilitate tastant access to the pharyngeal organs. The tissue sample was then carefully fixed in an inverted position in the pre-prepared well.

Adult hemolymph (AHL: 108 mM NaCl, 5 mM KCl, 8.2 mM $MgCl_2$, 2 mM $CaCl_2$, 4 mM $NaHCO_3$, 1 mM NaH_2PO_4, and 5 mM HEPES pH 7.5) was used as *Drosophila* imaging saline. After recording 1 minute as a pre-stimulus (20 µL AHL), we imaged the Ca^{2+} dynamics following the application of a specific tastant (5-fold higher concentration in 5 µL AHL). GCaMP6f fluorescence was observed using a fluorescence microscope (Axio Observer 3; Carl Zeiss) with a 20x objective, specifically focusing on the relevant area of the pharynx. Videos were recorded at a speed of two frames per second. Neuronal fluorescent activity changes were

recorded for 5 minutes following stimulus application. We did not use a perfusion system to wash the stimulus. Fiji/ImageJ software (https://fiji.sc) was used to measure fluorescence intensities. A region of interest (ROI) was drawn around the cell bodies, and the Time-Series Analyzer Plugin, developed by Balaji, J. (https://imagej.nih.gov/ij/plugins/time-series.html), was used to measure the average intensity for the ROIs during each frame. The average pre-stimulation value before chemical stimulation was calculated. ΔF/F (%) was determined using the formula $(F_{max}-F_0)/F_0 \times 100\%$, where F_0 represents the baseline value of GCaMP6f averaged for 10 frames immediately before stimulus application, and F_{max} is the maximum fluorescence value observed after stimulus delivery.

Statistical analyses

Error bars indicate the standard error of the means (SEMs), while the dots represent the number of trials conducted for the experiment. To compare multiple datasets, we used single-factor ANOVA coupled with Scheffe's analysis as a *post hoc* test. Pairwise comparisons were conducted using unpaired Student's *t*-tests. Statistical significance is denoted by asterisks (*$p < 0.05$, **$p < 0.01$). We performed all statistical analyses using Origin Pro 8 for Windows (ver. 8.0932; Origin Lab Corporation, USA).

Acknowledgments

This work was supported by grants to Y.L. from the National Research Foundation of Korea (NRF) funded by the Korea government (MIST) (NRF-2021R1A2C1007628)

and Biomaterials Specialized Graduate Program through the Korea Environmental Industry and Technology Institute (KEITI) funded by the Ministry of Environment (MOE), and grants to C.M. from the National Institute on Deafness and other Communication Disorders (NIDCD), R01-DC007864 and R01-DC016278. S.D., B.S., and D.N were supported by the Global Scholarship Program for Foreign Graduate Students at Kookmin University in Korea.

Additional information

Funding

Funder	Grant reference number	Author
National Research Foundation of Korea (NRF) funded by the Korea government (MIST)	NRF-2021R1A2C1007628	Youngseok Lee
National Institute on Deafness and other Communication Disorders (NIDCD)	R01-DC007864	Craig Montell
National Institute on Deafness and other Communication Disorders (NIDCD)	R01-DC016278	Craig Montell

Author contributions

J.S. and S.D. performed most of the genetic studies and physiology. J.S. and Y.L. conceived and designed the experiments. B.S. confirmed optogenetics and ectopic experiments. D.N. worked on low salt sensors. Y.K. generated most new reagents and conducted screening for high salt sensor in the initial stage. A.G. worked on the initial calcium imaging. C.M. and Y.L. supervised the project and wrote the manuscript.

Author ORCIDs

Jiun Sang https://orcid.org/0000-0002-0824-8428

Dhakal Subash https://orcid.org/0000-0002-5380-1130

Bhanu Shrestha https://orcid.org/0000-0002-2945-2305

Dharmendra Kumar Nath https://orcid.org/0000-0001-6105-6970

Yunjung Kim

Anindya Ganguly https://orcid.org/0000-0002-4798-0806

Craig Montell http://orcid.org/0000-0001-5637-1482

Youngseok Lee http://orcid.org/0000-0003-0459-1138

Additional files

Data availability

Source data for all figures contained in the manuscript and SI have been deposited in 'figshare' (https://doi.org/10.6084/m9.figshare.23939394).

Supplementary files

Figure 1—figure supplement 1. Requirements for *Ir*s for preferring low salt-containing food.

Figure 1—figure supplement 2. Gene structure of *Ir60b* locus, generation of *Ir60b*^{3} and behavioral defect of *Ir60b*^{1} in high salt avoidance.

Figure 2—figure supplement 1. Assaying action potentials induced by different labellar bristles in response to 300 mM salt using tip recordings.

Figure 2—figure supplement 2. Two-way solid-food choice assay to assess whether the *Gr2a*^{GAL4} mutant exhibits a deficit in avoidance of high salt.

Figure 3—figure supplement 1. DrosoX system and measurement of food intake using strychnine and coumarin.

Figure 3—figure supplement 2. Two-way solid-food choice assay and DrosoX binary capillary feeding assay using 100 mM sorbitol with or without 300 mM NaCl.

Figure 4—figure supplement 1. Testing whether ectopic expression of *Ir60b* confers responses to 300 mM NaCl, measurement of intake of sucrose plus 300 mM NaBr using the DrosoX assay, and Ca^{2+} response of *Ir60b* GRNs.

Figure 4—figure supplement 2. GCaMP6f responses evoked by 300 mM NaCl in *Ir60b* GRNs of control and $Ir7c^{GAL4}$ flies, and relative expression of *Ir60b* and *Ir7c* reporters in the LSO.

References

1. Heaney, R.P. (2006). Role of dietary sodium in osteoporosis. J. Am. Coll. Nutr. *25*, 271S-276S.
2. Jones, G., Beard, T., Parameswaran, V., Greenaway, T., and Von Witt, R. (1997). A population-based study of the relationship between salt intake, bone resorption and bone mass. Eur. J. Clin. Nutr. *51*, 561-565.
3. Luft, F., Rankin, L., Bloch, R., Weyman, A., Willis, L., Murray, R., Grim, C., and Weinberger, M. (1979). Cardiovascular and humoral responses to extremes of sodium intake in normal black and white men. Circ. J. *60*, 697-706.
4. Sharif, K., Amital, H., and Shoenfeld, Y. (2018). The role of dietary sodium in autoimmune diseases: The salty truth. Autoimmun. Rev. *17*, 1069-1073.
5. Strazzullo, P., D'Elia, L., Kandala, N.-B., and Cappuccio, F.P. (2009). Salt intake, stroke, and cardiovascular disease: meta-analysis of prospective studies. BMJ *339*.
6. Neal, B., Wu, Y., Feng, X., Zhang, R., Zhang, Y., Shi, J., Zhang, J., Tian, M., Huang, L., and Li, Z. (2021). Effect of salt substitution on cardiovascular events and death. N. Engl. J. Med. *385*, 1067-1077.
7. McDowell, S.A., Stanley, M., and Gordon, M.D. (2022). A molecular mechanism for high salt taste in *Drosophila*. Curr. Biol. *32*, 3070-3081. e3075.
8. Dweck, H.K., Talross, G.J., Luo, Y., Ebrahim, S.A., and Carlson, J.R. (2022). Ir56b is an atypical ionotropic receptor that underlies appetitive salt response in *Drosophila*. Curr. Biol. *32*, 1776-1787. e1774.
9. Dey, M., Ganguly, A., and Dahanukar, A. (2023). An inhibitory mechanism for suppressing high salt intake in *Drosophila*. Chem. Senses *48*, bjad014.

10. Lee, M.J., Sung, H.Y., Jo, H., Kim, H.-W., Choi, M.S., Kwon, J.Y., and Kang, K. (2017). Ionotropic Receptor 76b is required for gustatory aversion to excessive Na^+ in *Drosophila*. Mol. Cells *40*, 787.

11. Jaeger, A.H., Stanley, M., Weiss, Z.F., Musso, P.-Y., Chan, R.C., Zhang, H., Feldman-Kiss, D., and Gordon, M.D. (2018). A complex peripheral code for salt taste in *Drosophila*. Elife *7*, e37167.

12. Zhang, Y.V., Ni, J., and Montell, C. (2013). The molecular basis for attractive salt-taste coding in *Drosophila*. Science *340*, 1334-1338.

13. Nakamura, M., Baldwin, D., Hannaford, S., Palka, J., and Montell, C. (2002). Defective proboscis extension response (DPR), a member of the Ig superfamily required for the gustatory response to salt. J. Neurosci. *22*, 3463-3472.

14. Kim, H., Jeong, Y.T., Choi, M.S., Choi, J., Moon, S.J., and Kwon, J.Y. (2017). Involvement of a *Gr2a*-Expressing *Drosophila* pharyngeal gustatory receptor neuron in regulation of aversion to high-salt foods. Mol. Cells *40*, 331-338. 10.14348/molcells.2017.0028.

15. Montell, C. (2021). *Drosophila* sensory receptors—a set of molecular Swiss Army Knives. Genetics *217*, 1-34. 10.1093/genetics/iyaa011.

16. Wang, Z., Singhvi, A., Kong, P., and Scott, K. (2004). Taste representations in the *Drosophila* brain. Cell *117*, 981-991.

17. Thorne, N., Chromey, C., Bray, S., and Amrein, H. (2004). Taste perception and coding in *Drosophila*. Curr. Biol. *14*, 1065-1079.

18. Cameron, P., Hiroi, M., Ngai, J., and Scott, K. (2010). The molecular basis for water taste in *Drosophila*. Nature *465*, 91-95.

19. Lee, Y., Poudel, S., Kim, Y., Thakur, D., and Montell, C. (2018). Calcium taste avoidance in *Drosophila*. Neuron *97*, 67-74. e64.

20. Taisz, I., Dona, E., Munch, D., Bailey, S.N., Morris, B.J., Meechan, K.I., Stevens, K.M., Varela-Martinez, I., Gkantia, M., Schlegel, P., et al. (2023). Generating parallel representations of position and identity in the olfactory system. Cell *186*, 2556-2573 e2522. 10.1016/j.cell.2023.04.038.

21. Stanley, M., Ghosh, B., Weiss, Z.F., Christiaanse, J., and Gordon, M.D. (2021). Mechanisms of lactic acid gustatory attraction in *Drosophila*. Curr. Biol. *31*, 3525-3537. e3526.

22. Shrestha, B., and Lee, Y. (2021). Mechanisms of carboxylic acid attraction in *Drosophila melanogaster*. Mol. Cells *44*, 900.

23. Rimal, S., Sang, J., Poudel, S., Thakur, D., Montell, C., and Lee, Y. (2019). Mechanism of acetic acid gustatory repulsion in *Drosophila*. Cell Rep. *26*, 1432-1442. e1434.

24. Tauber, J.M., Brown, E.B., Li, Y., Yurgel, M.E., Masek, P., and Keene, A.C. (2017). A subset of sweet-sensing neurons identified by IR56d are necessary and sufficient for fatty acid taste. PLoS Genet. *13*, e1007059.

25. Brown, E.B., Shah, K.D., Palermo, J., Dey, M., Dahanukar, A., and Keene, A.C. (2021). Ir56d-dependent fatty acid responses in *Drosophila* uncover taste discrimination between different classes of fatty acids. Elife *10*, e67878.

26. Kim, H., Kim, H., Kwon, J.Y., Seo, J.T., Shin, D.M., and Moon, S.J. (2018). *Drosophila Gr64e* mediates fatty acid sensing via the phospholipase C pathway. PLoS Genet. *14*, e1007229.

27. Ahn, J.-E., Chen, Y., and Amrein, H. (2017). Molecular basis of fatty acid taste

in *Drosophila*. Elife *6*, e30115.

28. Aryal, B., Dhakal, S., Shrestha, B., and Lee, Y. (2022). Molecular and neuronal mechanisms for amino acid taste perception in the *Drosophila* labellum. Curr. Biol. *32*, 1376-1386. e1374.

29. Sánchez-Alcañiz, J.A., Silbering, A.F., Croset, V., Zappia, G., Sivasubramaniam, A.K., Abuin, L., Sahai, S.Y., Münch, D., Steck, K., and Auer, T.O. (2018). An expression atlas of variant ionotropic glutamate receptors identifies a molecular basis of carbonation sensing. Nat. Commun *9*, 4252.

30. Alves, G., Sallé, J., Chaudy, S., Dupas, S., and Manière, G. (2014). High-NaCl perception in *Drosophila melanogaster*. J. Neurosci. *34*, 10884-10891.

31. Liu, L., Leonard, A.S., Motto, D.G., Feller, M.A., Price, M.P., Johnson, W.A., and Welsh, M.J. (2003). Contribution of *Drosophila* DEG/ENaC genes to salt taste. Neuron *39*, 133-146.

32. Chen, Y.D., and Dahanukar, A. (2017). Molecular and cellular organization of taste neurons in adult *Drosophila* pharynx. Cell Rep. *21*, 2978-2991. 10.1016/j.celrep.2017.11.041.

33. Chen, Y.D., and Dahanukar, A. (2020). Recent advances in the genetic basis of taste detection in *Drosophila*. Cell Mol Life Sci *77*, 1087-1101. 10.1007/s00018-019-03320-0.

34. Stocker, R.F. (1994). The organization of the chemosensory system in *Drosophila melanogaster*: a review. Cell Tissue Res. *275*, 3-26.

35. Nayak, S.V., and Singh, R.N. (1983). Sensilla on the tarsal segments and mouthparts of adult *Drosophila melanogaster* meigen (Diptera, Drosophilidae). Int. J. Insect Morphol. Embryol. *12*, 273-291. Doi 10.1016/0020-

7322(83)90023-5.

36. LeDue, E.E., Chen, Y.C., Jung, A.Y., Dahanukar, A., and Gordon, M.D. (2015). Pharyngeal sense organs drive robust sugar consumption in *Drosophila*. Nat. Commun. *6*, 6667. 10.1038/ncomms7667.

37. Joseph, R.M., and Heberlein, U. (2012). Tissue-specific activation of a single gustatory receptor produces opposing behavioral responses in *Drosophila*. Genetics *192*, 521-532. 10.1534/genetics.112.142455.

38. Xiao, S., Baik, L.S., Shang, X., and Carlson, J.R. (2022). Meeting a threat of the Anthropocene: Taste avoidance of metal ions by *Drosophila*. Proc. Natl. Acad. Sci. U.S.A. *119*, e2204238119. 10.1073/pnas.2204238119.

39. Soldano, A., Alpizar, Y.A., Boonen, B., Franco, L., Lopez-Requena, A., Liu, G., Mora, N., Yaksi, E., Voets, T., Vennekens, R., et al. (2016). Gustatory-mediated avoidance of bacterial lipopolysaccharides via TRPA1 activation in *Drosophila*. eLife *5*. 10.7554/eLife.13133.

40. Choi, J., van Giesen, L., Choi, M.S., Kang, K., Sprecher, S.G., and Kwon, J.Y. (2016). A pair of pharyngeal gustatory receptor neurons regulates caffeine-dependent ingestion in *Drosophila* larvae. Front Cell Neurosci *10*, 181. 10.3389/fncel.2016.00181.

41. Chen, Y.D., Menon, V., Joseph, R.M., and Dahanukar, A.A. (2021). Control of sugar and amino acid feeding via pharyngeal taste neurons. J Neurosci *41*, 5791-5808. 10.1523/JNEUROSCI.1794-20.2021.

42. Joseph, R.M., Sun, J.S., Tam, E., and Carlson, J.R. (2017). A receptor and neuron that activate a circuit limiting sucrose consumption. Elife *6*, e24992.

43. Caterina, M.J., Schumacher, M.A., Tominaga, M., Rosen, T.A., Levine, J.D.,

and Julius, D. (1997). The capsaicin receptor: a heat-activated ion channel in the pain pathway. Nature *389*, 816-824. 10.1038/39807.

44. Sang, J., Dhakal, S., and Lee, Y. (2021). Cucurbitacin B suppresses hyperglycemia associated with a high sugar diet and promotes sleep in *Drosophila melanogaster*. Mol. Cells *44*, 68.

45. Marella, S., Fischler, W., Kong, P., Asgarian, S., Rueckert, E., and Scott, K. (2006). Imaging taste responses in the fly brain reveals a functional map of taste category and behavior. Neuron *49*, 285-295.

46. Klapoetke, N.C., Murata, Y., Kim, S.S., Pulver, S.R., Birdsey-Benson, A., Cho, Y.K., Morimoto, T.K., Chuong, A.S., Carpenter, E.J., and Tian, Z. (2014). Independent optical excitation of distinct neural populations. Nat. Methods *11*, 338-346.

47. Nitabach, M.N., Blau, J., and Holmes, T.C. (2002). Electrical silencing of *Drosophila* pacemaker neurons stops the free-running circadian clock. Cell *109*, 485-495.

48. Dahanukar, A., Lei, Y.-T., Kwon, J.Y., and Carlson, J.R. (2007). Two Gr genes underlie sugar reception in *Drosophila*. Neuron *56*, 503-516.

49. Dambly-Chaudière, C., Jamet, E., Burri, M., Bopp, D., Basler, K., Hafen, E., Dumont, N., Spielmann, P., Ghysen, A., and Noll, M. (1992). The paired box gene *pox neuro*: A determiant of poly-innervated sense organs in *Drosophila*. Cell *69*, 159-172.

50. Fujita, M., and Tanimura, T. (2011). *Drosophila* evaluates and learns the nutritional value of sugars. Curr. Biol. *21*, 751-755.

51. Burke, C.J., and Waddell, S. (2011). Remembering nutrient quality of sugar in

Drosophila. Curr. Biol. *21*, 746-750.

52. Moon, S.J., Lee, Y., Jiao, Y., and Montell, C. (2009). A *Drosophila* gustatory receptor essential for aversive taste and inhibiting male-to-male courtship. Curr. Biol. *19*, 1623-1627.

53. Li, X., Sun, Y., Gao, S., Li, Y., Liu, L., and Zhu, Y. (2023). Taste coding of heavy metal ion-induced avoidance in *Drosophila*. iScience *26*, 106607. 10.1016/j.isci.2023.106607.

54. Yang, T., Yuan, Z., Liu, C., Liu, T., and Zhang, W. (2021). A neural circuit integrates pharyngeal sensation to control feeding. Cell Rep. *37*.

55. Rop, O., Sochor, J., Jurikova, T., Zitka, O., Skutkova, H., Mlcek, J., Salas, P., Krska, B., Babula, P., Adam, V., et al. (2010). Effect of five different stages of ripening on chemical compounds in medlar (Mespilus germanica L.). Molecules *16*, 74-91. 10.3390/molecules16010074.

56. Taruno, A., and Gordon, M.D. (2023). Molecular and cellular mechanisms of salt taste. Annu. Rev. Physiol. *85*, 25-45.

57. Benton, R., Vannice, K.S., Gomez-Diaz, C., and Vosshall, L.B. (2009). Variant ionotropic glutamate receptors as chemosensory receptors in *Drosophila*. Cell *136*, 149-162.

58. Thistle, R., Cameron, P., Ghorayshi, A., Dennison, L., and Scott, K. (2012). Contact chemoreceptors mediate male-male repulsion and male-female attraction during *Drosophila* courtship. Cell *149*, 1140-1151. 10.1016/j.cell.2012.03.045.

59. Gong, W.J., and Golic, K.G. (2003). Ends-out, or replacement, gene targeting in *Drosophila*. Proc. Natl. Acad. Sci. USA *100*, 2556-2561.

60. Brand, A.H., and Perrimon, N. (1993). Targeted gene expression as a means of altering cell fates and generating dominant phenotypes. Development *118*, 401-415.

61. Aryal, B., Dhakal, S., Shrestha, B., Sang, J., Pradhan, R.N., and Lee, Y. (2022). Protocol for binary food choice assays using *Drosophila melanogaster*. STAR protocols *3*, 101410.

62. Lee, Y., Moon, S.J., Wang, Y., and Montell, C. (2015). A *Drosophila* gustatory receptor required for strychnine sensation. Chem. Senses *40*, 525-533.

63. Yapici, N., Cohn, R., Schusterreiter, C., Ruta, V., and Vosshall, L.B. (2016). A taste circuit that regulates ingestion by integrating food and hunger signals. Cell *165*, 715-729.

64. Lee, Y., Moon, S.J., and Montell, C. (2009). Multiple gustatory receptors required for the caffeine response in *Drosophila*. Proc. Natl. Acad. Sci. U.S.A. *106*, 4495-4500.

65. Weiss, L.A., Dahanukar, A., Kwon, J.Y., Banerjee, D., and Carlson, J.R. (2011). The molecular and cellular basis of bitter taste in *Drosophila*. Neuron *69*, 258-272.

66. Lee, Y., and Montell, C. (2013). *Drosophila* TRPA1 functions in temperature control of circadian rhythm in pacemaker neurons. J. Neurosci. *33*, 6716-6725.

67. Inagaki, H.K., Jung, Y., Hoopfer, E.D., Wong, A.M., Mishra, N., Lin, J.Y., Tsien, R.Y., and Anderson, D.J. (2014). Optogenetic control of *Drosophila* using a red-shifted channelrhodopsin reveals experience-dependent influences on courtship. Nat. Methods *11*, 325-332.

857

858

Figure legends

Figure 1. Testing requirements for *Ir*s for avoiding high salt-containing food, and chemogenetic and optogenetic control of *Ir60b* GRNs. (**A**) Binary food choice assays (1 mM sucrose versus 5 mM sucrose and 300 mM NaCl) comparing 30 *Ir* mutants to the control strain (w^{1118}) for high salt avoidance, n=8–12. (**B**) Preferences of the indicated flies for 1 mM sucrose versus 5 mM sucrose and 0—1000 mM NaCl. n=8–12. (**C**) Testing the effects of 100 μM capsaicin after expressing the rat TRPV1 channel (*UAS-trpV1*) either in Class A GRNs or *Ir60b* GRNs under the control of the *Gr64f-GAL4* or the *Ir60b-GAL4*, respectively. The flies were given a choice between 2 mM sucrose or 2 mM sucrose plus 100 μM capsaicin. The presence or absence of the various transgenes is indicated by "+" and "-", respectively. n=8. (**D**) Testing the effects of light activation of various classes of GRNs. *UAS-CsChrimson* was expressed in Class A GRNs (driven by the *Gr5a-GAL4*), Class B GRNs (driven by the *Gr66a-GAL4*) or in *Ir60b* GRNs (driven by the *Ir60b-GAL4*). The flies were then simultaneously exposed to red lights (650 nm; WP-5700, 3M, USA) for 5 sec while 2% sucrose was applied to labellum and the percent PER was recorded. n=6. Data were compared using single-factor ANOVA coupled with Scheffe's *post hoc* test. Statistical significance compared with the control. Means ± SEMs. **$p < 0.01$.

Figure 2. Contributions of different classes of GRNs to high salt avoidance. (**A**) Schematic showing the names of sensilla bristles on the labellum [65]. (**B**) Tip recordings conducted on S3, S7, and L3 sensilla using 300 mM NaCl and the indicated flies. n=10–16. (**C**) Representative traces obtained from S3 sensilla. (**D**)

Binary food choice assays (1 mM sucrose versus 5 mM sucrose and 300 mM NaCl) after inactivating different classes of GRNs with *UAS-Kir2.1*, driven by the indicated *GAL4* drivers: Class A (*Gr64f*; blue), Class B (*Gr66a*; red), Class C (*ppk28*; green) and Class D (*ppk23*; purple). Significances were determined by comparing to the *UAS-Kir2.1* only control (black). n=12. (**E**) Tip recordings conducted by stimulating S3 and S7 sensilla with 300 mM NaCl from flies with different classes of GRNs inactivated with *UAS-Kir2.1*. See panel **D** for legend. n=16–20. (**F—I**) PER assays performed using the control strain (w^{1118}; black) and $Ir25a^{2}$ (red), $Ir60b^{3}$ (blue), $Ir76b^{1}$ (green). n=8–10. (**F**) PER percentages induced by 2% sucrose (1st offering). (**G**) PER percentages induced by 2% sucrose (2nd offering). (**H**) PER percentages induced by 2% sucrose with 300 mM NaCl (1st offering). (**I**) PER percentages induced by 2% sucrose with 300 mM NaCl (2nd offering). (**J**) Binary food choice assays for 300 mM salt avoidance were conducted with the control strain, *Poxn* ($Poxn^{70\text{-}28}/Poxn^{\Delta M22\text{-}B5}$), $Ir25a^{2}$, $Ir60b^{3}$, $Ir76b^{1}$, and $Poxn;Ir60b^{3}$. n=9–12. Data were compared using single-factor ANOVA coupled with Scheffe's *post hoc* test. Statistical significances compared with the control flies or the *Poxn* mutant are denoted by black and red asterisks, respectively. Means ± SEMs. **$p < 0.01$.

Figure 3. Measuring volume of food intake in *Ir* mutants using the DrosoX system. **(A—N)** Each fly was exposed to two capillaries, one of which contained 100 mM sucrose (a), and the other contained 100 mM sucrose and 300 mM NaCl (b). (**O and P**) Each fly was exposed to two capillaries, one of which contained 100 mM sucrose (c), and the other contained 100 mM sucrose and 10 mM caffeine (d). (**A, C, E, G, I, K, M** and **O**) Volumes of the two food options consumed by the indicated flies over

the course of 6 hrs. (**B, D, F, H, I, J, L, N** and **P**) Ingestion indexes to indicate the relative consumption of the two foods. Ingestion indexes were calculated in each time point using the following equation: [(Ingestion volume of 100 mM sucrose and 300 mM NaCl or 10 mM caffeine)-(Ingestion volume of 100 mM sucrose)]/[(Ingestion volume of 100 mM sucrose and 300 mM NaCl or 10 mM caffeine)+(Ingestion volume of 100 mM sucrose)] n=12. Multiple sets of data were compared using single-factor ANOVA coupled with Scheffe's *post hoc* test. Statistical significances were relative to the control and determined for the Ingestion indexes only. In all panels, the controls were w^{1118}. The colors of the asterisks match the colors of the genotypes in the corresponding panels. Means ± SEMs. **$p < 0.01$.

Figure 4. GCaMP6f responses of *Ir60b* GRNs to NaCl and other chemicals. (**A**) Relative staining of the *Ir60b* reporter (green, anti-GFP) and the *Ir76b* reporter (red; anti-dsRed) in the LSO of *UAS-mCD8*::*GFP*/*Ir76b-QF2*;*Ir60b-GAL4*/*QUAS-tdTomato* flies. Merge is to the right. (**B**) Relative staining of the *Ir25a* reporter (green, anti-GFP) and the *Ir76b* reporter (red; anti-dsRed) in the LSO of *Ir25a-GAL4*/*Ir76b-QF2*;*UAS-mCD8*::*GFP*/*QUAS-tdTomato*. Merge is to the right. (**C—J**) Peak GCaMP6f responses (ΔF/F) of *Ir60b* GRNs in flies expressing *UAS-GCaMP6f* under control of the indicated *GAL4* driver. (**C**) Heat map images illustrating changes in GCaMP6f fluorescence before and after stimulation with 300 mM NaCl using the indicated flies. (**D**) Sample traces depicting GCaMP6f responses to 300 mM NaCl. The traces are from the indicated flies expressing *UAS-GCaMP6f* driven by the *Ir60b-GAL4*. n=10–14. (**E**) GCaMP6f responses to various concentrations of NaCl in the indicated flies. *UAS-GCaMP6f* was driven by the *Ir60b-GAL4*. n=10–14. (**F**) GCaMP6f responses to

300 mM NaCl in the indicated mutants and in the absence or presence of the corresponding rescue transgene indicated by "-" and "+", respectively. n=8–10. (**G**) GCaMP6f responses to 50 mM, 300 mM, and 500 mM of $CaCl_2$, $MgCl_2$, and KCl in control flies. n=10–14. (**H**) GCaMP6f responses of *Ir60b* GRNs from the indicated flies to various concentrations of NaBr. n=10–14. (**I**) GCaMP6f responses to 5 mM and 50 mM concentrations of bitter compounds (quinine, caffeine, strychnine, lobeline, denatonium, and coumarin). n=8–10. (**J**) GCaMP6f responses to various concentrations of sucrose in *Ir60b* GRNs from the indicated flies. n=10–14. Multiple sets of data were compared using single-factor ANOVA coupled with Scheffe's *post hoc* test. Statistical significance compared with the controls. Means ± SEMs. **$p < 0.01$.

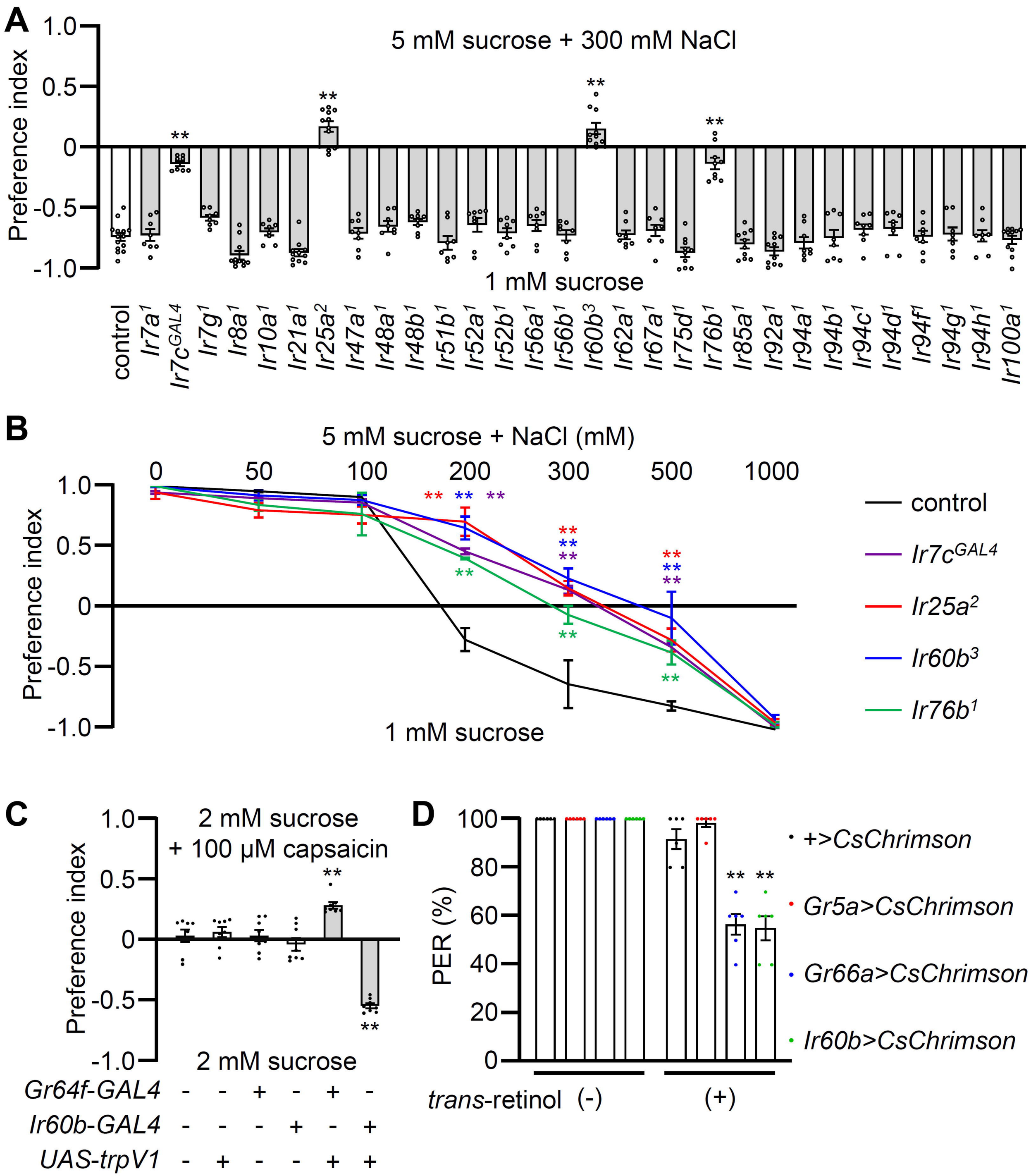
A
5 mM sucrose + 300 mM NaCl
Preference index
1.0
0.5
0
-0.5
-1.0
1 mM sucrose
control
Ir7a1
Ir7cGAL4
Ir7g1
Ir8a1
Ir10a1
Ir21a1
Ir25a2
Ir47a1
Ir48a1
Ir48b1
Ir51b1
Ir52a1
Ir52b1
Ir56a1
Ir56b1
Ir60b3
Ir62a1
Ir67a1
Ir75d1
Ir76b1
Ir85a1
Ir92a1
Ir94a1
Ir94b1
Ir94c1
Ir94d1
Ir94f1
Ir94g1
Ir94h1
Ir100a1
B
5 mM sucrose + NaCl (mM)
0
50
100
200
300
500
1000
Preference index
1 mM sucrose
control
Ir7cGAL4
Ir25a2
Ir60b3
Ir76b1
C
2 mM sucrose
+ 100 μM capsaicin
Preference index
2 mM sucrose
Gr64f-GAL4 - - + - + -
Ir60b-GAL4 - - - + - +
UAS-trpV1 - + - - + +
D
PER (%)
100
80
60
40
20
0
trans-retinol (-) (+)
+>CsChrimson
Gr5a>CsChrimson
Gr66a>CsChrimson
Ir60b>CsChrimson

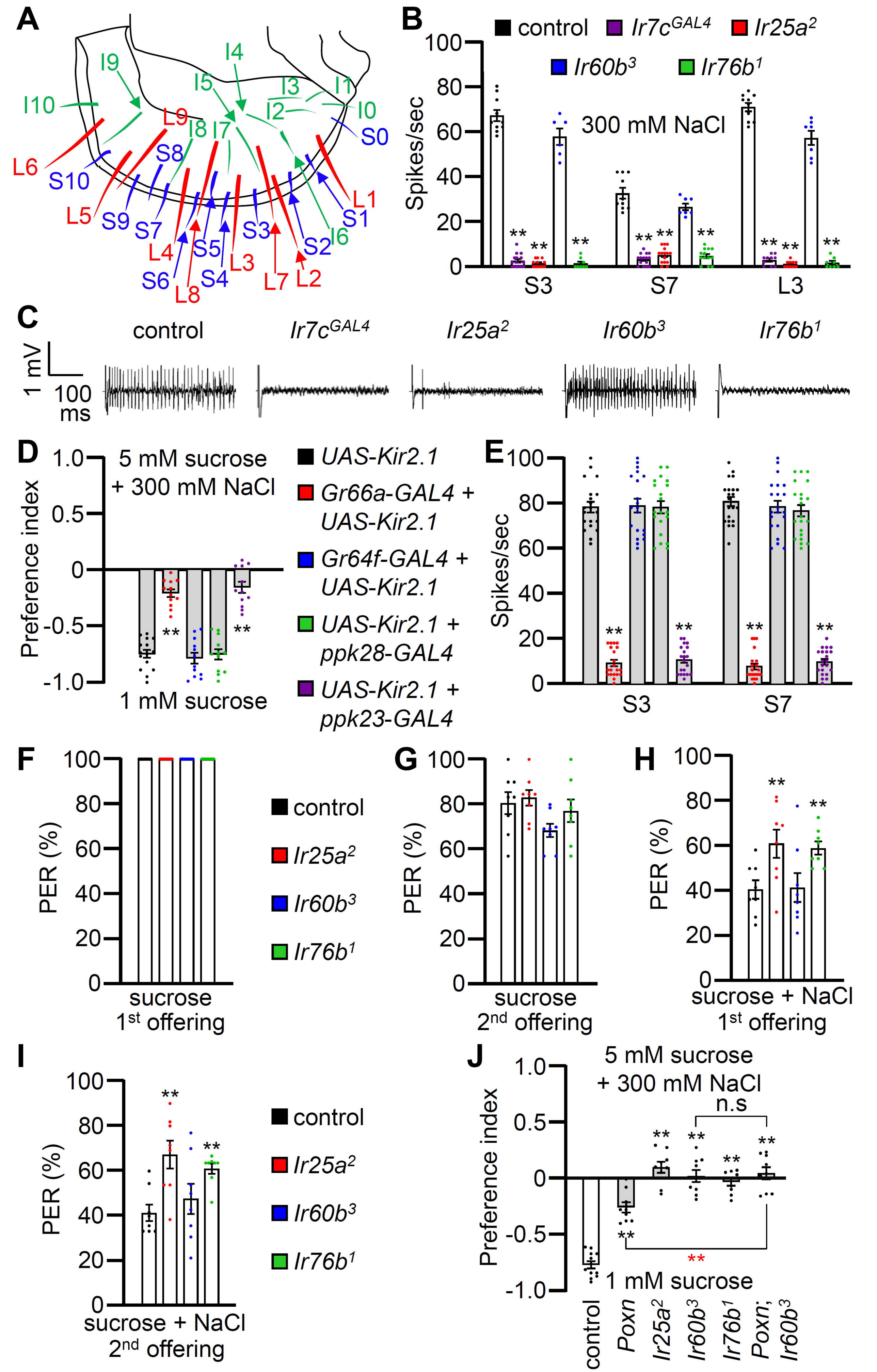
A
I9
I4
I5
I3
I1
I10
I2
I0
L9
I8
I7
S0
L6
S8
S10
L1
L5
S9
S7
S1
S3
I6
L4
S5
S2
L3
S6
S4
L7
L2
L8
B
control
Ir7c GAL4
Ir25a 2
Ir60b 3
Ir76b 1
300 mM NaCl
Spikes/sec
S3
S7
L3
C
control
Ir7c GAL4
Ir25a 2
Ir60b 3
Ir76b 1
1 mV
100 ms
D
5 mM sucrose
+ 300 mM NaCl
Preference index
1 mM sucrose
UAS-Kir2.1
Gr66a-GAL4 + UAS-Kir2.1
Gr64f-GAL4 + UAS-Kir2.1
UAS-Kir2.1 + ppk28-GAL4
UAS-Kir2.1 + ppk23-GAL4
E
Spikes/sec
S3
S7
F
PER (%)
sucrose
1st offering
control
Ir25a 2
Ir60b 3
Ir76b 1
G
PER (%)
sucrose
2nd offering
H
PER (%)
sucrose + NaCl
1st offering
I
PER (%)
sucrose + NaCl
2nd offering
control
Ir25a 2
Ir60b 3
Ir76b 1
J
5 mM sucrose
+ 300 mM NaCl
n.s
Preference index
1 mM sucrose
control
Poxn
Ir25a 2
Ir60b 3
Ir76b 1
Poxn; Ir60b 3

(a, dark color) 100 mM sucrose alone
(b, light color) 100 mM sucrose + 300 mM NaCl

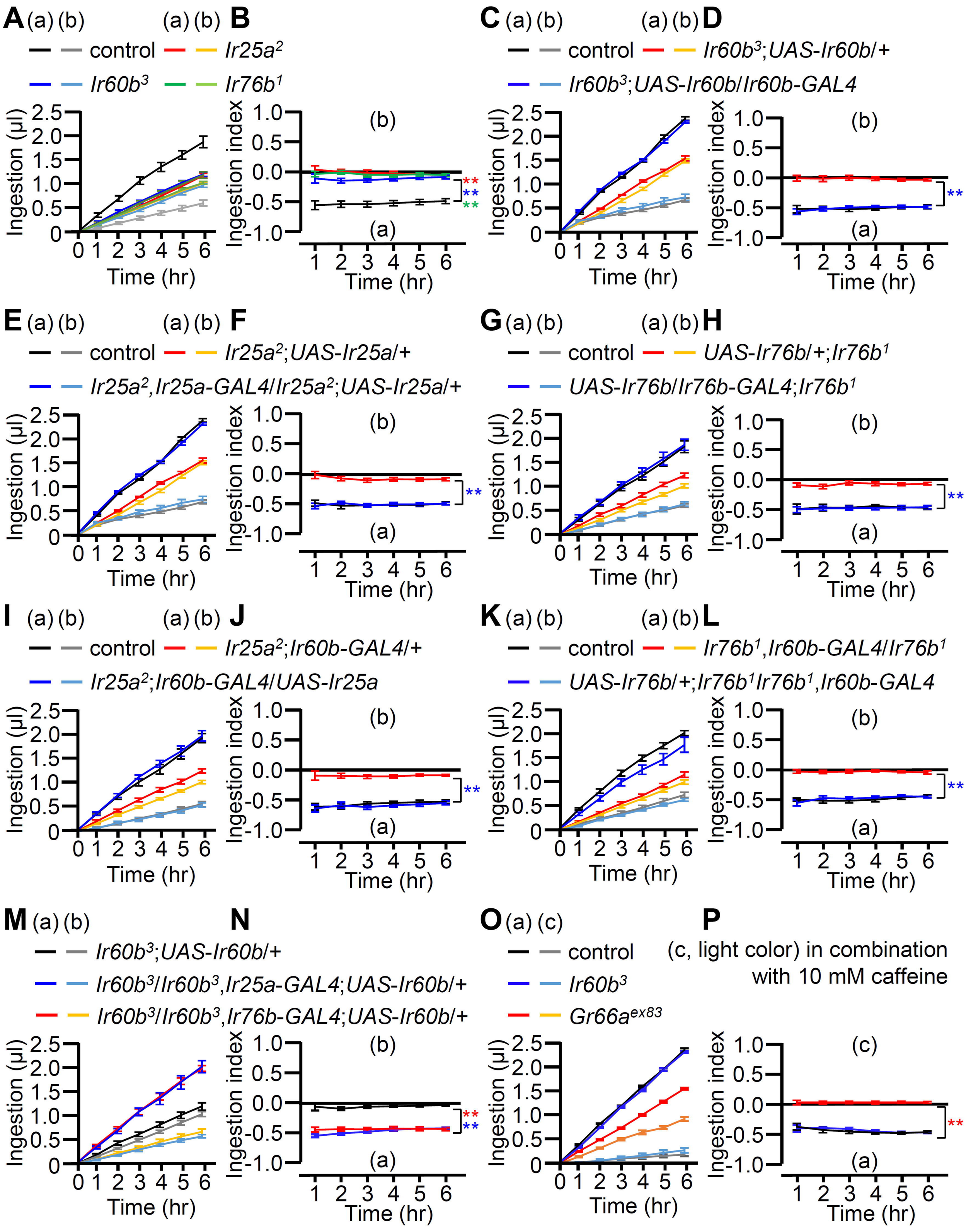

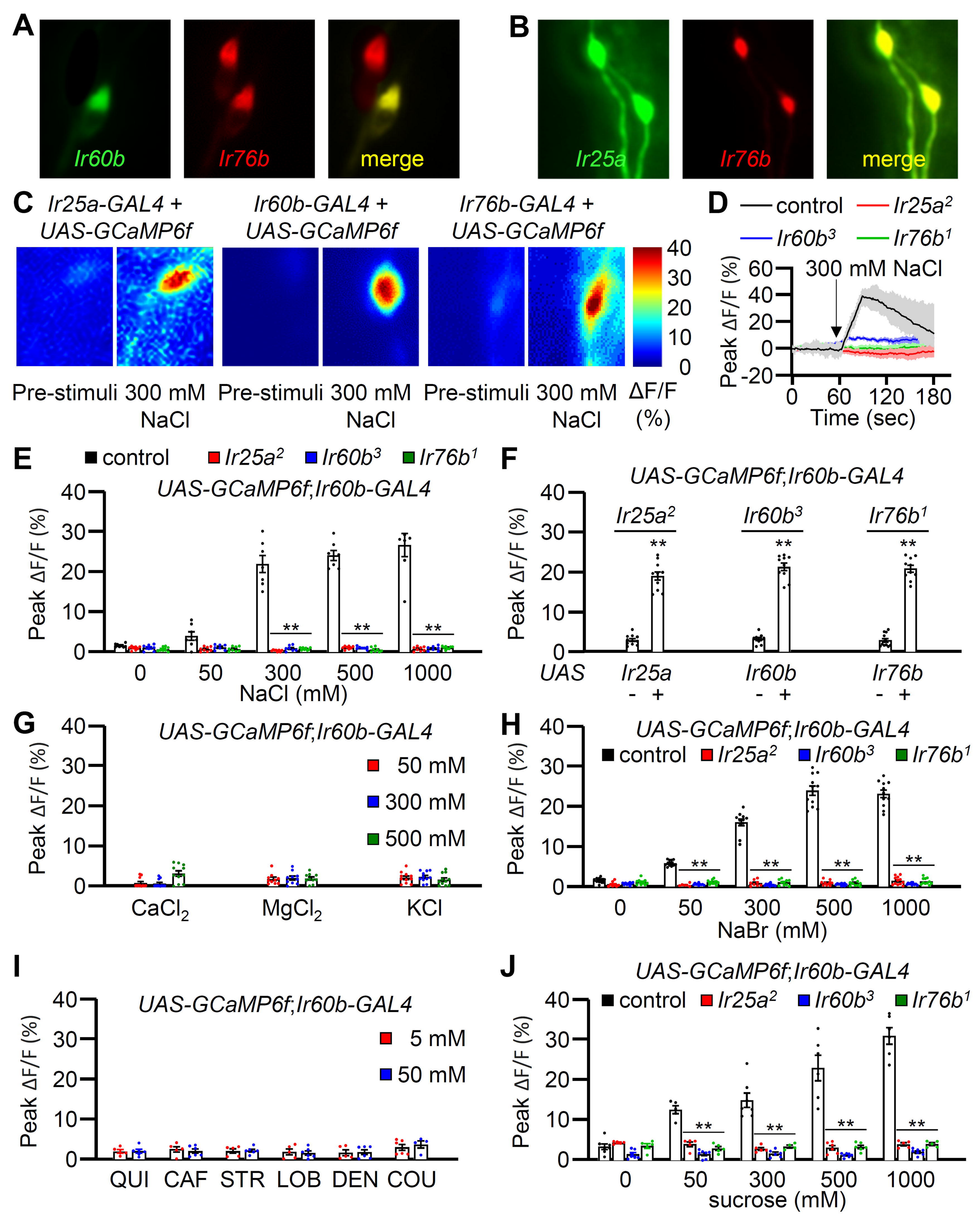
A
Ir60b
Ir76b
merge
B
Ir25a
Ir76b
merge
C
Ir25a-GAL4 + UAS-GCaMP6f
Ir60b-GAL4 + UAS-GCaMP6f
Ir76b-GAL4 + UAS-GCaMP6f
Pre-stimuli
300 mM NaCl
ΔF/F (%)
D
control
Ir25a2
Ir60b3
Ir76b1
300 mM NaCl
Peak ΔF/F (%)
Time (sec)
E
control
Ir25a2
Ir60b3
Ir76b1
UAS-GCaMP6f;Ir60b-GAL4
Peak ΔF/F (%)
NaCl (mM)
F
UAS-GCaMP6f;Ir60b-GAL4
Ir25a2
Ir60b3
Ir76b1
UAS
Ir25a
Ir60b
Ir76b
G
UAS-GCaMP6f;Ir60b-GAL4
50 mM
300 mM
500 mM
CaCl2
MgCl2
KCl
H
UAS-GCaMP6f;Ir60b-GAL4
control
Ir25a2
Ir60b3
Ir76b1
NaBr (mM)
I
UAS-GCaMP6f;Ir60b-GAL4
5 mM
50 mM
QUI
CAF
STR
LOB
DEN
COU
J
UAS-GCaMP6f;Ir60b-GAL4
control
Ir25a2
Ir60b3
Ir76b1
sucrose (mM)